23.0 Atomic Resonance and Scattering

Academic and Research Staff

Prof. D. Kleppner, Prof. D.E. Pritchard

Visiting Scientist

T.W. Ducas[1]

Postdoctoral Associates

G.P. Lafyatis, A.G. Martin

Graduate Students

V.S. Bagnato, K. Boyce, P.P. Chang, E.A. Cornell, T.J. Gentile, K. Helmerson, L. Hsu, B. Hughey, C-H. Iu, M.M. Kash, D.W. Keith, B.G. Oldaker, S. Paine, E.L. Raab, R.E. Stoner, R.M. Weiskoff, G.R. Welch

Undergraduate Students

D. Lew, J. Landry, A.H. Miklich, G. Zeglin

23.1 Basic Atomic Physics

23.1.1 Rydberg Atoms in a Magnetic Field

National Science Foundation (Grant PHY 87-06560)

Michael M. Kash, George R. Welch, Chun-Ho Iu, Long Hsu, Daniel Kleppner

We have produced Rydberg atoms in a lithium atomic beam using cw dye lasers, developed the technology for cw detection of these atoms with static electric field ionization, and performed accurate measurement of the atomic energy levels in a strong magnetic field. A procedure for determining accurately the magnetic field strength has been implemented. These measurements allow the characterization of important spectral features, including the size and location of level anticrossings.

Understanding the diamagnetic spectrum of an atom with a single valence electron presents a formidable challenge to theory and experiment.[1] The quantum mechanical equations of motion are easily constructed, but in spite of the simplicity of the problem the solutions are elusive and our understanding is far from complete. Numerical techniques have been developed that are accurate for relatively low energy and field. However, even in this regime, these calculations provide little insight into the physics

---

1 Wellesley College

of the anticrossings. The widely held view is that *hydrogen* atomic energy levels very nearly cross, so lithium anticrossings are a manifestation of the valence electron - atomic core interaction.[2] Our measurements provide a one-hundred fold increase in accuracy over previous studies,[3] so any model of the core can be tested strenuously.

The excitation of iithium Rydberg atoms is performed with a two-step, three-photon process. The first step is a two-photon transition from the 2s to the 3s state. This step is detected by observing the cascade fluorescence (3s → 2p, 2p → 2s) through a fiber optic bundle with a sensitive photomultiplier tube. The transition is excited by 735 nm light from a ring dye laser. The 2p → 2s fluorescence is used to stabilize the laser against slow drift. The second step is a one-photon transition from the 3s state to the *n*p state, accomplished with radiation from a second ring dye laser. This resonance is observed by counting electrons which are produced in ionizing the excited atoms as they move from the interaction volume into a region of static electric field, 5-10kV/cm. The electrons are counted with a surface barrier diode. Standard devices such as electron multiplier tubes, channeltron multipliers, or micro-channel plates do not operate in a strong magnetic field (greater than 1 Tesla).

To minimize the electric field in the atom's rest frame, an atomic beam of lithium is used with velocity parallel to the axis of a superconducting solenoid. The interaction region consists of an aluminum cylinder whose axis is parallel to the atomic beam. The cylinder also contains prisms to deflect the lasers so that the laser and atomic beams intersect at right angles, to minimize Doppler broadening. The interaction region combines efficient collection of cascade fluorescence with good geometric rejection of scattered laser light. Measurement of the magnetic field uses the linear Zeeman effect: the energy difference between corresponding states with $m = +1$ and $m = -1$ is equal to the Bohr magneton times the field. With this technique, the field can be determined to about 20 gauss.

Figure 23.1 shows a theoretical prediction of energy levels in atomic lithium as a function of magnetic field with $m=0$, odd parity, near $n=25$. The three indicated anticrossings have been experimentally studied. The first anticrossing data are displayed in figure 23.2. The data are generated by fixing the magnetic field and scanning the second laser over the indicated energy range. The anticrossing is a manifestation of perturbations to the hydrogenic Hamiltonian by the non-hydrogenic potential within lithium core electrons. The decrease of transition probability in the upper state reveals that this state is an antisymmetric combination of hydrogen states, while the lower state is a symmetric combination. The resonance linewidth is about 30 MHz. In figure 23.3 the theory and experiment are compared. The anticrossing size is the minimum energy separation of the two levels; the anticrossing position is the field location of this minimum. These are determined by fitting a hyperbola to the data. The experimental uncertainty in the position of anticrossings 1 and 3 is reduced over that of 2 because we improved the field measurement technique: for 2 we had only a magneto-resistor probe. The agreement between theory and experiment of anticrossing location seems reasonable, but in the case of anticrossing 1, there appears to be a small but real discrepancy. This is probably caused by a stray electric field in the interaction region.

In the next phase of the research we plan to extend the study of anticrossings and to expand our spectroscopic survey to study global properties of the system including the evolution of the spectrum from regions of orderly to disorderly classical motion.

23.1.2 Microwave Quantum Optics

Joint Services Electronics Program (Contract DAAL03-86-K-0002)

Theodore W. Ducas, Thomas J. Gentile, Barbara Hughey, Daniel Kleppner

The interaction of an atom with electromagnetic fields, including the vacuum field, is modified by conducting surfaces. A cavity tuned to an atomic transition will enhance the absorption and emission rates of that transition above their free space values. If the cavity damping time is long (high Q), there can be an oscillatory exchange of energy between the atom and the cavity. An experiment is in progress to study these effects using Rydberg states of calcium in the TM010 mode of a cylindrical superconducting cavity at 35 GHz.

An atomic beam of calcium is generated by a tube oven and a collimating aperture. Rydberg states of calcium are produced by a three-step pulsed laser excitation. A Quanta-Ray DCR-1A Nd:Yag laser is used to pump three dye lasers. The first dye laser drives the 4s4s → 4s4p transition at 423 nm. The second step is the 4s4p → 4s5s transition at 1035 nm. The 1035 nm light is produced by generating the difference frequency of a dye laser (525 nm) and the Nd:Yag fundamental (1064 nm) in a KD*P crystal. Finally the third laser drives the 4s5s → 4snp transition. By tuning the wavelength of the third laser, nearly any 4snp Rydberg state can be excited.

Calcium was chosen for this experiment because its dominant isotope (calcium 40, 97% abundance) has no hyperfine structure. Moreover, calcium has two valence electrons which can combine into either a singlet or a triplet state. By choosing the singlet state, we also avoid fine structure. This allows us to have a true two-level system for the cavity experiment.

The atomic transition we have chosen for this experiment is 46p → 46s. Rydberg states ionize in modest electric fields; a particular Rydberg state can be identified by the value of the electric field required for ionization. This technique is used to resolve the two Rydberg states involved in the transition. We use ramped electric field plates that ionize the two states at distinct positions along the atomic beam direction. The ramp is optimized for the 46p → 46s transition, but can be used for a variety of Rydberg state transitions. The electrons released by the ionization are detected by channel electron multipliers, which generate a distinct electrical pulse for each detected electron. Consequently, we can count the number of atoms in the two Rydberg states involved in the transition.

The oscillatory exchange of energy between the atom and the cavity can be destroyed by the presence of blackbody radiation at the transition frequency. For this reason, and also to achieve a sufficiently high Q using a superconducting cavity, this experiment is carried out at low temperatures. To achieve this goal, the interaction region of the apparatus is attached to the bottom of a liquid helium dewar. We expect to reach 1.5 degrees Kelvin by lowering the pressure above the helium bath. We have recently modified the dewar apparatus and achieved the following goals: improved microwave and electrical access to the apparatus; better cryogenic design; installation of the channel electron multipliers and magnetic shielding; and greater overall flexibility and convenience.

We have performed preliminary experiments in which Rydberg state transitions are driven by a high resolution microwave source. The source is an HP 8690B sweep oscillator locked to an HP 8662A synthesizer. These experiments have allowed us to test the resolution of the detector. In addition, we have accurately measured the frequency of the 46p → 46s transition, which is necessary for the design of the cavity. The study of these microwave transitions is also an excellent diagnostic for systematic problems in our apparatus. Because of the extreme sensitivity of Rydberg atoms, small electric fields can broaden the spectral linewidth of the transition and destroy the coherent exchange of energy between the atom and the cavity. The measurement of the spectral linewidth of the Rydberg state transitions and the observation of coherent effects have allowed us to diagnose and reduce stray electric fields. The reduction of stray electric fields is directly related to the cleanliness of the vacuum system and to the alignment and properties of the lasers. Figure 23.4 shows a frequency scan of the microwave source over the 46p → 46s transition. The observed linewidth of 300 kHz is dominated by the transit time across the waveguide in which the transition occurs. Since our system is so well suited to measuring the transition frequencies of these Rydberg state transitions, we plan to measure a variety of transition frequencies in calcium. We expect these measurements to have a resolution of approximately 10^6. Figures 23.5 and 23.6 are examples of coherent phenomena that we have studied. Figure 23.5 shows the evolution of the magnetic sublevels of the 46p state in the ambient magnetic field. (This field will be greatly reduced by shielding in the cavity experiment, but its presence is useful for these diagnostic experiments.) Figure 23.6 shows the dependence of the Rabi oscillation frequency on microwave power with and without the magnetic shielding. In the presence of microwaves tuned to the Rydberg state transition frequency, the atomic population will oscillate between the two Rydberg states involved in the transition. These oscillations are reminiscent of the coherent exchange of energy between the atom and the cavity.

The cavity mode that we have chosen is the TM010 mode of a right circular cylindrical cavity because the electric field in this mode is constant along the length of the cavity. The atoms travel parallel to the cavity axis, and the constant electric field simplifies the analysis of our experiment. Another advantage of this mode is that it allows us to conveniently probe the time dependence of the atom-cavity interaction. With the TM010 mode, the cavity can be split lengthwise into two halves without greatly perturbing the mode structure. We can then electrically isolate the two halves and apply a small voltage to one half at various times during the atom-cavity interaction. This small dc electric field shifts the atomic resonance away from the cavity resonance, thus stopping the atom-cavity interaction and "freezing" the atomic population. This enables us to trace out the oscillation of the atomic population between the 46p and 46s states in the cavity. The split cavity can be tuned by varying the size of the gap between the halves. To achieve $Q>10^7$ in the split cavity we must minimize the leakage of microwaves out of the crack separating the halves. This is accomplished by machining a small "choke" groove around the cavity.

The cavity is analyzed by coupling it to a waveguide through a small aperture and detecting the reflected power from the cavity as a function of frequency. The locked, narrowband microwave system described above is necessary to observe these high Q cavities (for $Q=10^7$, the source needs to be stable to better than 500 Hz). The properties of the decrease in the reflected power near resonance are used to determine the intrinsic Q of the cavity, Q_0.

A vacuum chamber with a small liquid helium dewar is used to test the cavities. The pressure above the helium is reduced in order to lower the temperature of the cavity to less than 1.8K. Figure 23.7 shows the measured Q as a function of temperature of a lead-plated copper split cavity with a choke groove. The Q increases exponentially as the temperature decreases, as is predicted by the BCS theory for superconductors. Work is in progress to tune this cavity while maintaining a high Q.

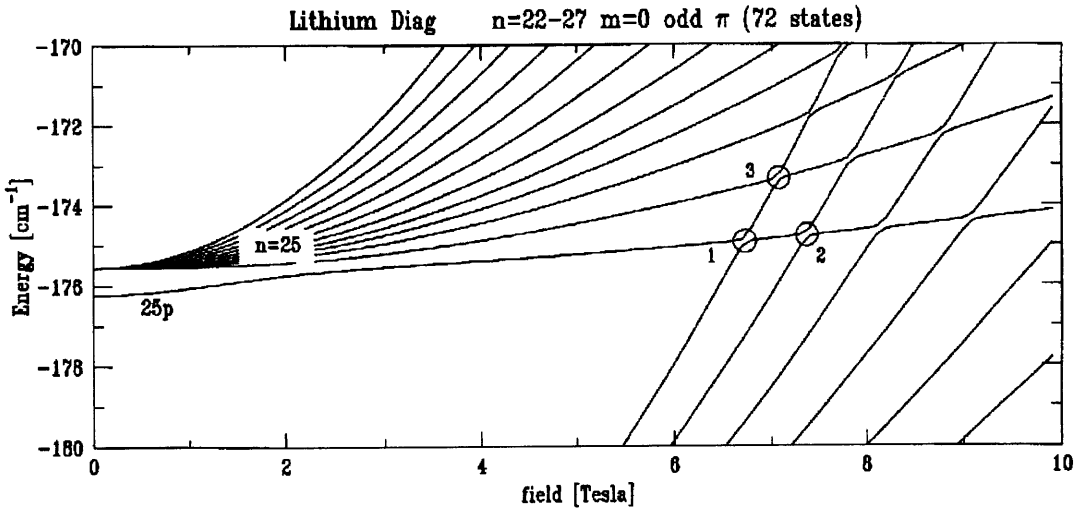

Figure 23.1 Theoretical prediction of atomic lithium energy levels with m=0, odd parity near n=25.

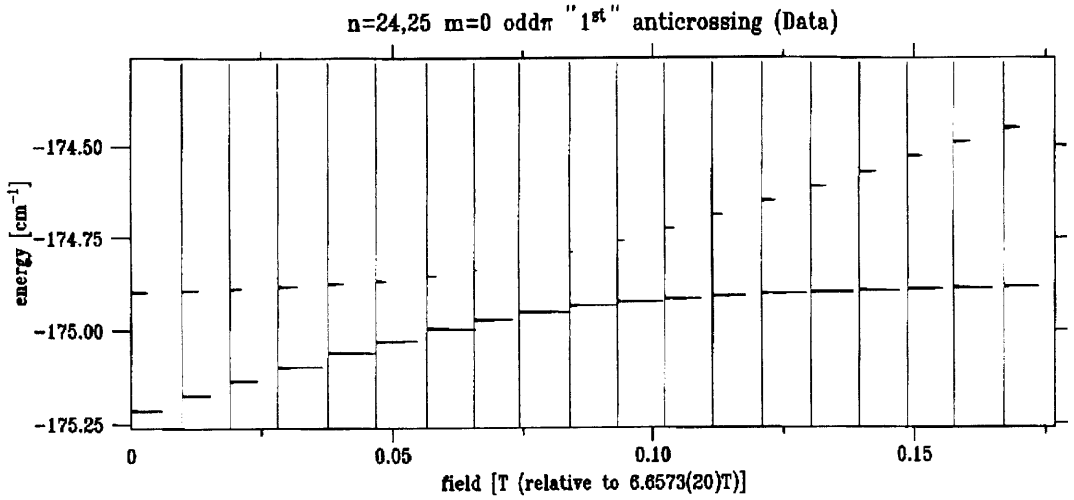

Figure 23.2 Experimental study of anticrossing 1. The baseline of each laser scan determines the magnetic field. The base of each resonance is the energy of the state at the corresponding field.

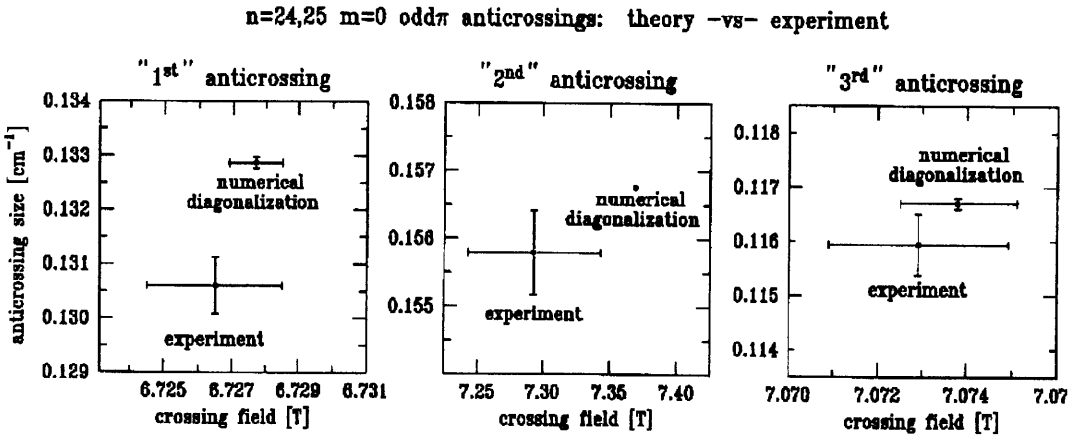

Figure 23.3 Comparison of theory and experiment. The bars on the theory indicate the extent of convergence in the calculation.

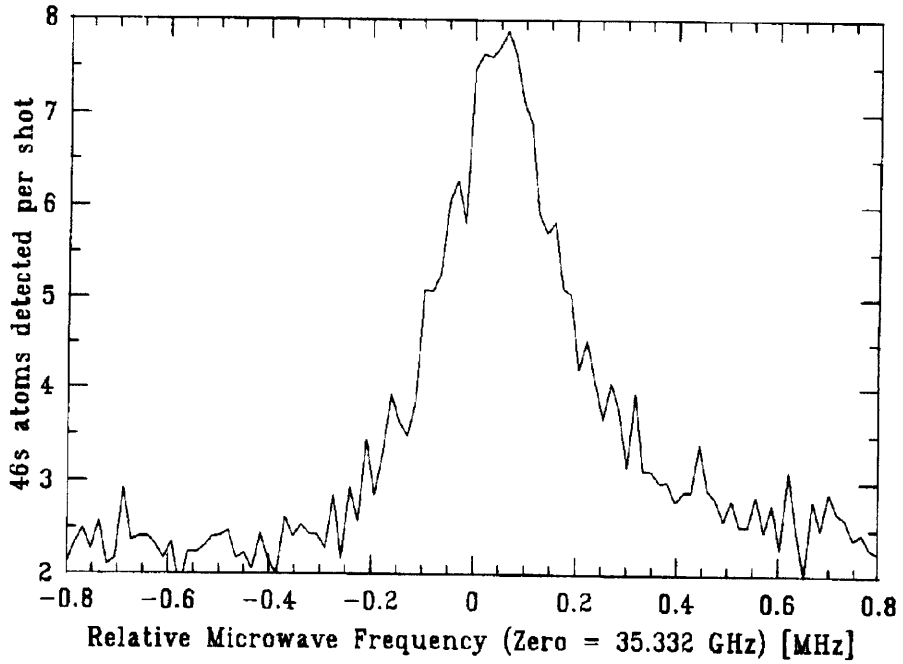

Figure 23.4. Low power frequency scan of the microwave source over the calcium 46p → 46s transition. Power is ~ 10^{-14} Watts.

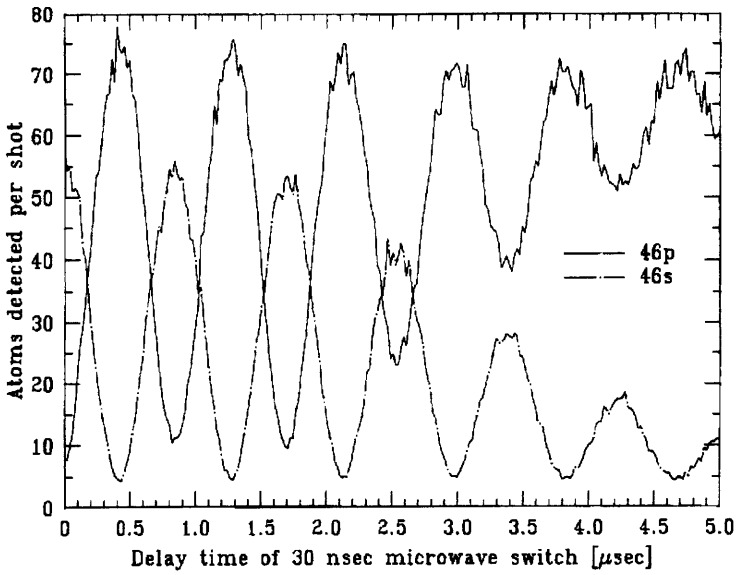

Figure 23.5 M-level evolution in the ambient magnetic field of 0.42 gauss. The 46p atoms reflect the population in the 46p $m = \pm -1$ states and the 46s atoms reflect the population in the 46p m=0 state before the 30 nsec microwave switch is applied.

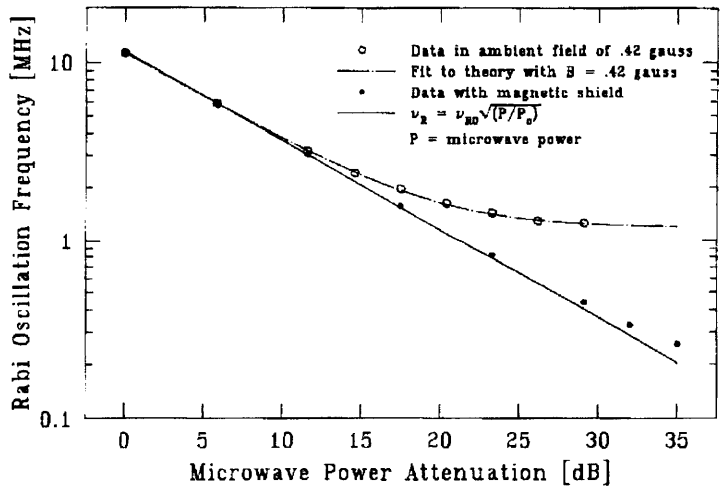

Figure 23.6 Rabi oscillation frequency of the calcium $46p \rightarrow 46s$ transition as a function of microwave power. The data were taken with and without the magnetic shield. The solid curve is $\nu_R \propto$ microwave electric field strength. The dashed line is a fit to the observed oscillation frequency in the presence of the magnetic field: $\nu_{osc} = \sqrt{\nu_R^2 + 4\nu_L^2}$ where ν_L is the Larmor frequency.

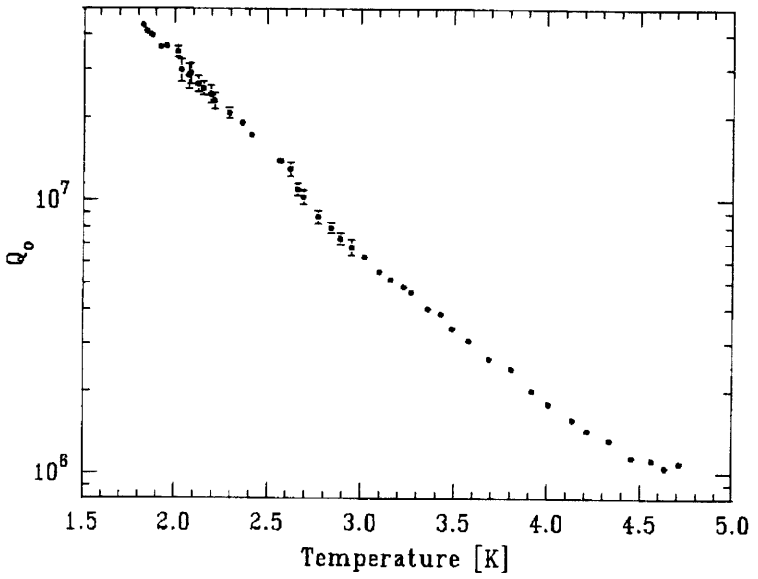

Figure 23.7 Unloaded Q of TM_{010} mode of a lead plated split cavity as a function of temperature.

23.1.3 Millimeter Wave Measurements of Rydberg Constant

National Science Foundation (Grant PHY 87-06560)

Pin P. Chang, Scott Paine, Daniel Kleppner

We are undertaking a determination of the Rydberg constant of hydrogen by measuring the frequency of the transition $n = 29 \rightarrow n = 30$, at 256 GHz. Our approach differs from that of previous determinations in that the Rydberg is measured in frequency units. This avoids the problems of wavelength metrology that limit optical measurements. The design goal is an accuracy of 1 part in 10^{11}, approximately thirty times higher than optical measurements.

We have started construction of an atomic beam apparatus, and have carried out preliminary studies on the optical excitation of Rydberg atoms. Our first goal will be to prepare the atoms in "circular" states using a novel method recently proposed by Delande and Gay.[4]

References

[1] J.C. Gay, "High Magnetic Field Atomic Physics." In *Progress in Atomic Spectroscopy,* eds. H.J. Beyer and H. Kleinpoppen. New York: Plenum, 1984.

[2] M.L. Zimmerman, M.M. Kash, and G.R. Welch, *J. Phys.* 43:C2-113 (1982).

[3] P. Cacciani, E. Luc-Koenig, J. Pinard, C. Thomas, and S. Liberman, *J. Phys. B* 19:L519 (1986).

[4] D. Delande and J.C. Gay, *Europhys. Lett.* 5:303 (1988).

23.2 Magnetic Trap for Neutral Atoms

Joint Services Electronics Program (Contract DAAL03-86-K-0002)
U.S. Navy - Office of Naval Research (Contract N00014-83-K-0695)

Vanderlei S. Bagnato, Gregory P. Lafyatis, Alexander G. Martin, Kristian Helmerson, David E. Pritchard, Joseph Landry

We are working on a program to trap large numbers of atoms and cool them to microkelvin temperatures. The objective - a dense sample of ultra cold atoms - promises to open up new and exciting areas of physics. The lack of interaction of the trapped atoms with any confining walls, their low velocities due to their reduced thermal motion, and the possibility of indefinitely long interaction times makes such samples of trapped atoms ideal for high resolution spectroscopy and for use as atomic frequency standards. High density samples of ultra-cold atoms also promise to open up new areas of research in the study of both interatomic collisions and collective effects, such as Bose condensation.

Following the completion and successful demonstration of our superconducting magnetic trap for neutral atoms in 1986,[1] we have worked to elevate neutral traps from laboratory curiosities to powerful tools for new research in physics.

Our chief accomplishments in 1987 include: trapping greater numbers of atoms; inducing R.F. transitions amongst the various magnetic substates; and doppler cooling of the atoms to milli-kelvin temperatures.

We have succeeded in trapping $\sim 2 \times 10^{10}$ Na atoms. This is a sufficient number of atoms to make the sample optically dense, so that up to 60% of a weak probe beam is absorbed during one pass through the sample. Figure 23.8 (a) shows a typical absorption spectrum of trapped atoms. The shape of the absorption spectrum reflects the longitudinal magnetic field profile.[1]

We have also doppler-cooled the trapped atoms. A laser beam is sent down the axis of the trap and retro-reflected back on itself. Tuned to the red of the atomic transition frequency the standing wave forms a one-dimensional version of "optical molasses".[2] In this manner, we have succeeded in cooling our sample to approximately 4 mK. Figure 23.8 (b) shows a typical absorption spectrum of doppler cooled atoms. The increase (decrease) in the absorption at the low (high) frequency side of the curve corresponds to an increase (decrease) in the density of atoms at the low (high) magnetic field values (they have been sufficiently cooled so that they no longer have enough energy to reach the high magnetic field region).

Our greatest success in 1987 was the first observation of R.F. induced transitions on trapped atoms. With the application of R.F. we have succeeded in transferring the populations among the various ground state hyperfine levels of sodium, which we de-

tect through fluorescence induced by a weak probe laser beam. Figure 23.9 (a) shows a typical fluorescence spectrum of trapped atoms taken just after loading the trap. The atoms are in the F=2, M=2 hyperfine level, the state selected by our slowing and stopping lasers. Figure 23.9 (b) is a fluorescence spectrum of trapped atoms after repeated application of R.F. pulses to induce transitions from the initial F=2, M=2 to F=2, M=1,0,-1 hyperfine levels. Each of the peaks corresponds to one of these four ground state hyperfine levels, shifted in frequency by the presence of the external magnetic field, the only states in which weak-field seeking atoms can be trapped.

In addition, we have obtained a R.F. resonance curve for the F=2, M=2 to F=2, M=1 transition by measuring the relative peak heights of the two states in the fluorescence spectrum as a function of the frequency of the applied R.F. pulse. Figure 23.10 is such a curve. A fit to the curve from a model indicates the temperature of the atoms to be $\sim$ 60mK These first observations of R.F. transitions on trapped atoms are of great interest, not only because they provide us with a measurement of the temperature of our atoms, but also because they are essential to a scheme which we have proposed to cool atoms to micro-kelvin temperatures using combined R.F. optical techniques.[3] Such supercooling is the key to both high resolution spectroscopy and collective effects.

References

[1] V.S. Bagnato, G.P. Lafyatis, A.G. Martin, E.L. Raab, R.N. Ahmad-Bitar, D.E. Pritchard, *Phys. Rev. Lett.* 58:2194 (1987).

[2] S. Chu, L. Hollberg, J.E. Bjorkholm, A. Cable, and A. Ashkin, *Phys. Rev. Lett.* 55:48 (1985).

[3] D.E. Pritchard, *Phys. Rev. Lett.* 54:1336 (1983).

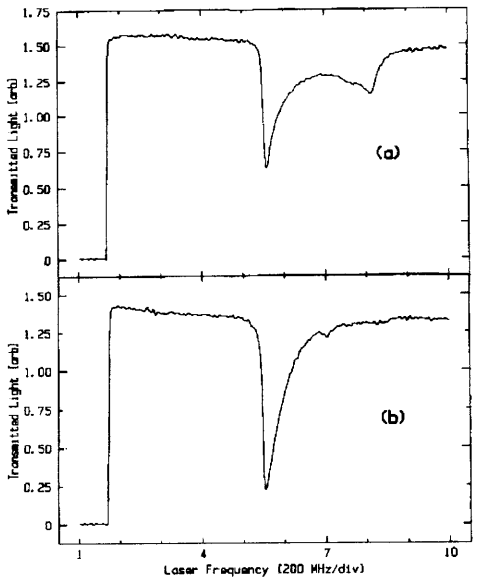

Figure 23.8 (a) Absorption spectrum of magnetically trapped sodium atoms taken just after loading of trap.

23.8 (b) Absorption spectrum taken after application of doppler cooling.

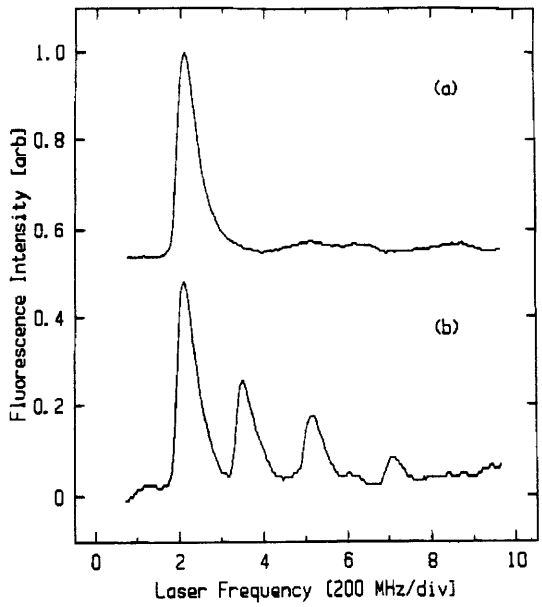

Figure 23.9 (a) is a fluorescence spectrum of atoms trapped in the F=2, M=2 state.

23.9 (b) is a spectrum showing population in all four trapped magnetic substates, F=2, M=2,1,0,-1.

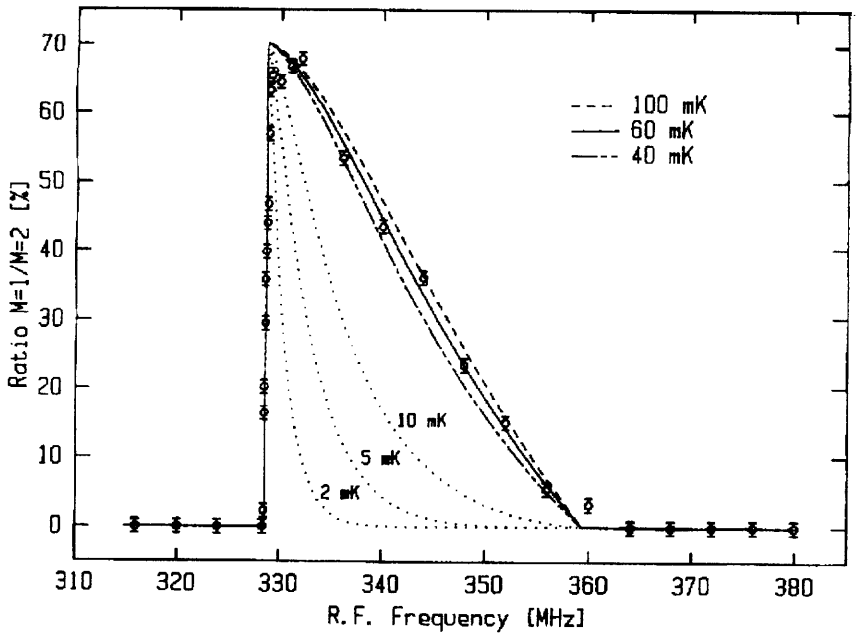

Figure 23.10 is a R.F. resonance lineshape (points) for the F=2, M=1 to F=2, M=2 transition. The calculated lineshapes (curves) allow us to estimate the temperature of the trapped atoms. The calculations for 2,5 and 10 mK show the greatly increased sensitivity to temperature for colder samples.

23.2.1 Light Trap

Joint Services Electronics Program (Contract DAAL03-83-K-0002)
U.S. Navy - Office of Naval Research (Grant N00014-83-K-0695)

Alexander G. Martin, Eric L. Raab, Richard E. Stoner, Debra Lew, David E. Pritchard

We are constructing an apparatus to slow, confine, and cool neutral atoms with laser light. The apparatus will enable us to produce clouds of $>10^8$ sodium or lithium atoms with temperatures of less than 500 μk and densities of $>10^{11}$atoms/cm^3. With these cold, dense gases we will study long range molecules,[1] associative ionization,[2]

$$(Na^* + Na^* \rightarrow Na_2^+ + e^-)^2, \tag{1}$$

and low-energy collision processes.

Low-energy collisions provide challenges to both theorist and experimentalist because the duration of an ultra-cold excited-state collision is several natural lifetimes! Such a collision process, in which a spontaneous decay is probable, has yet to be observed or modeled.

In 1987 we demonstrated the first spontaneous force light trap in experiments at Bell Laboratories in collaboration with Mara Prentiss, Alex Cable, and Steve Chu.[3] This trap relies on the use of a magnetic field to induce the atoms to preferentially absorb light propagating towards trap center.[4] In this experiment we trapped over 10^7 neutral atoms for over 2 minutes in a trap with a confinement volume of several cm^3 and a depth >0.4K. The density of atoms was about 2x10^{11}atoms/cm^3; the temperature was ap-

proximately 600 μk. The observation of escape of atoms from the trap (inferred from the decay of the fluorescence from the trap, figure 23.11) revealed a loss mechanism manifest at high densities proportional to the square of the density of trapped atoms.

Figure 23.12 depicts the new MIT apparatus. Atoms coming up through the dewar bottom will be slowed by a laser beam propagating counter to the atomic beam. A tapered solenoid superconducting magnet (the "slower" of figure 23.12) creates a Zeeman shift of the atomic levels which compensates for the changing Doppler shift of the atoms as they decelerate. Three pairs of counterpropagating laser beams intersecting at the center of the "anti-Helmholtz" trap coils (i.e., two coils oriented coaxially with oppositely-directed dipole moments) comprise the trap (figure 23.13).

The continuous loading capability to be afforded by the tapered solenoid slower, as well as the high central field gradient attainable by the superconducting trap coils, will afford us a significant improvement in density over that of the Bell Laboratories trap. The improved vacuum resulting from the LHe dewar cryo-pumping should substantially increase the trap lifetime. The new apparatus will be operational by mid-1988.

References

[1] W. Stwalley, *Contemp. Phys.* 19:65 (1979).

[2] P. Gould et al., to be published.

[3] E. Raab et al., *Phys. Rev. Lett.* 59:109 (1987).

[4] D.E. Pritchard et al., *Phys. Rev. Lett.* 57:310 (1986); the particular trap demonstrated at Bell Laboratories grew out of discussions with J. Dalibard.

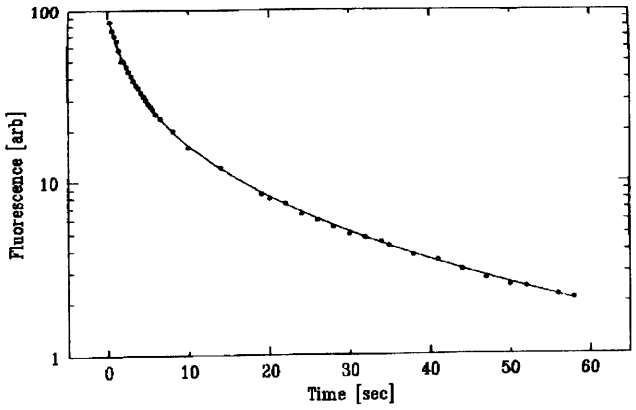

Figure 23.11 Decay of the fluorescence from the trapped atoms when the initial density was high. We see that at early times, the decay deviates from a simple exponential, indicating the presence of non-linear decay. The solid line represents a fit of Eq. (1) to the data.

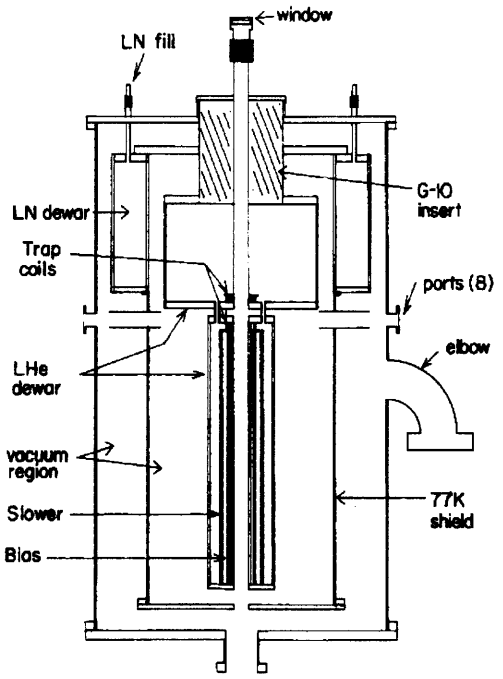

Figure 23.12 Schematic of apparatus.

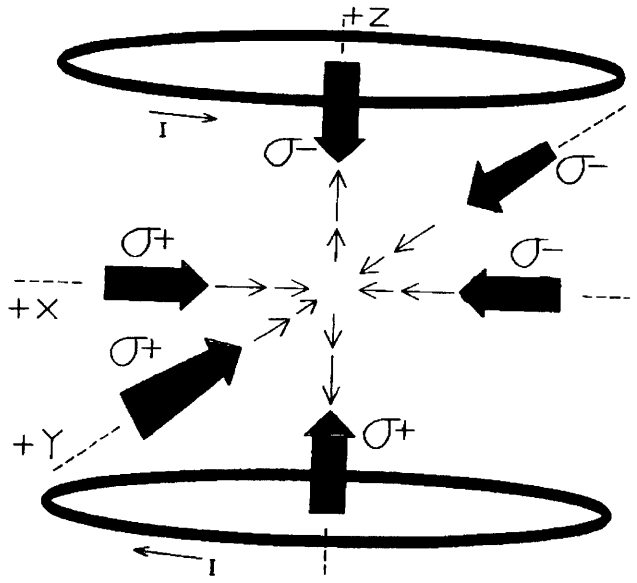

Figure 23.13. Trapping scheme in three dimensions. The "spherical quadrupole" field is generated by two coils of opposing current placed along the z-axis approximately as shown. The field along the axes, indicated by the light arrows is parallel to its respective axis. Laser light, indicated by the heavy arrows, counter-propagates along x, y, z and is polarized as shown with respect to the axis of propagation.

23.2.2 Atom Wave Interferometer

Joint Services Electronics Program (Contract DAAL03-86-K-0002)
National Science Foundation (Grant PHY 86-05893)

David W. Keith, Bruce G. Oldaker, Garth Zeglin, David E. Pritchard

We are beginning a program to make an atom interferometer (one which interferes atomic deBroglie waves). In order to realize such a device on needs components analogous to those employed in conventional optics. We are currently investigating different technologies that could serve as elements of an "atomic optical" system. Two sorts of atomic optical elements are contemplated; those that exert forces on atoms through their interaction with near-resonant light, and grazing incidence diffraction gratings or micro fabricated transmission optics designed for x-rays of comparable wavelengths.

The key component for an interferometer is a coherent beam splitter. In 1986 our group was the first to demonstrate an atomic beam splitter.[1] We used the near resonant Kapitza-Dirac effect in which an atom is diffracted through a standing wave of laser light. However, this technique has several disadvantages, it requires a complex, stabilized laser and results in very small beam separations, on the order of 10^{-4} rads. In addition, such a technique is limited to atoms that have easily accessible laser transitions, which are not the atomic species most suitable for many conceivable applications of atom interferometers.

The observation of specular reflection of thermal alkali atoms from surfaces at grazing incidence[2] implies the possibility of observing diffraction of our atomic beam from a x-ray diffraction grating designed for comparable wavelengths. Gratings have been demonstrated for x-rays with wavelengths below 1 Å; they produce diffracted angles in the order of 10^{-2} rad. This technology would be ideal for use as an atomic beam splitter. Gratings are cheap and reliable (compared to lasers), and they could produce much larger angular beam separations resulting in more compact or sensitive interferometers. We have constructed an addition to our existing high resolution sodium beam machine to allow us to investigate grazing incidence reflections. During the last few months we have tested two simple gratings.

Interferometers measure the difference in the phase accumulated by particles traveling between two points by spatially separated paths. Thus an interferometer is sensitive to length changes caused by absolute rotation or relative mechanical displacements of its parts, as well as to energy shifts caused by electromagnetic or gravitational interactions. To date interferometers have been made for photons and neutrons. For almost all purposes atoms would be better for matter wave interferometers than neutrons. Atoms are far more sensitive to electromagnetic interactions, they are available with ~ 10 times shorter wavelengths, and from cheap compact sources (neutrons come from reactors). The fluxes available in atomic beams are 10^8 times larger than those for neutrons; high fluxes would enable an atomic interferometer to make use of the fringe splitting techniques developed for optical interferometers. An atomic interferometer is intrinsically 10^5 times more sensitive to mechanical displacement than an optical interferometer. Since atoms travel many times slower than light, atomic interferometers are 10^{10} more sensitive to rotations than laser gyros. Atomic interferometers could be used to make precise measurements of atomic properties as well as to make funda-

mental tests in physics including Berry's phase, and the phase shift on rotation of bosons and fermions.

References

[1] A. Anderson, S. Haroche, E.A. Hinds, W. Jhe, D. Meschede, and L. Moi, *Phys. Rev. A* 34:3513 (1986).

[2] P.L. Gould, G.A. Ruff, and D.E. Pritchard, *Phys. Rev. Lett.* 56:827 (1986).

23.2.3 Precision Mass Spectroscopy of Ions

Joint Services Electronics Program (Contract DAAL03-86-K-0002)
National Science Foundation (Grant PHY 86-05893)

Kevin R. Boyce, Eric A. Cornell, Gregory P. Lafyatis, David E. Pritchard, Robert M. Weisskoff

We are developing an experiment to determine the mass of individual atomic and molecular ions at precisions of 10^{-11}. This technique will allow us to do a variety of experiments which address issues of both fundamental and applied physics:

- The $^3H^+ - {}^3He^+$ mass difference is an important parameter in ongoing experiments to measure the electron neutrino rest mass.
- Excitation and binding energies of typical atomic and molecular ions might be studied by "weighing" the small increase in energy: $\Delta m = E_{bind}/c^2$.
- Experiments that weigh γ-rays can be used in a new method to determine Avogadro's number, N_A, a key fundamental constant.
- Traditional applications of mass spectroscopy should benefit from the several orders of magnitude improvement in both accuracy and the sensitivity our approach offers over conventional techniques.

We will measure ratios of cyclotron frequencies, and therefore masses, of a small number of atomic or molecular ions in a Penning trap at 4.2K. To attain the precision we seek, it will be necessary to work with only one, or at most two ions in the trap. Space charge from other ions would lead to undesirable frequency shifts. Thus or mass spectrometer will have the ultimate sensitivity - a single molecule.

We will use ion trapping techniques based on methods developed at the University of Washington, where they have made precision measurements on protons, electrons and positrons at the 10^{-11} level. Trapped ions are detected by the small currents which they induce in the trap electrodes as they move. However, because atomic and molecular ions have larger masses, and thus lower resonant frequencies, they induce much smaller currents than the particles studied at Washington. Consequently, we developed a detector using a SQUID (Superconducting QUantum Interference Device) and superconducting electronics to measure these small induced currents, typically $< 10^{-14}$A.

This year, following several improvements on the apparatus and the detector,[1] we began systematic high-precision measurements on small clouds of ions (typically $\sim 5 - 10 N_2^+$ ions) stored in our trap. We learned how to minimize the non-harmonic electric fields, and, in addition, how to cool the trapped ions so that the remaining perturbations have smaller effects. We have used these cooled ions to make our first precision cyclotron measurements using a novel "avoided-crossing" technique.

Figure 23.14 shows a typical example of compensation decreasing the anharmonicity of the trap. The asymmetry in the left and right peaks come from a quartic term in the trapping potential. In the center peak, we have minimized this term using an additional set of electrodes in the trap. C_4 is a measure of the size of the quartic term.)

Figure 23.15 is an avoided-crossing cyclotron measurement. For this measurement, we have coupled the axial and cyclotron modes together with an inhomogeneous electric field, oscillating near their difference frequency, $\nu_c' - \nu_z$. When resonant, this electric field splits the axial mode. Figure 23.15 yields a 5×10^{-8} measurement of the cyclotron frequency and, in addition, provides information about the strength of the coupling field.

In the coming year, we expect to observe these effects with single ions and continue precision measurement work.

Reference

[1] R. Weisskoff et al., *J. Appl. Phys.* 63:4599 (1988).

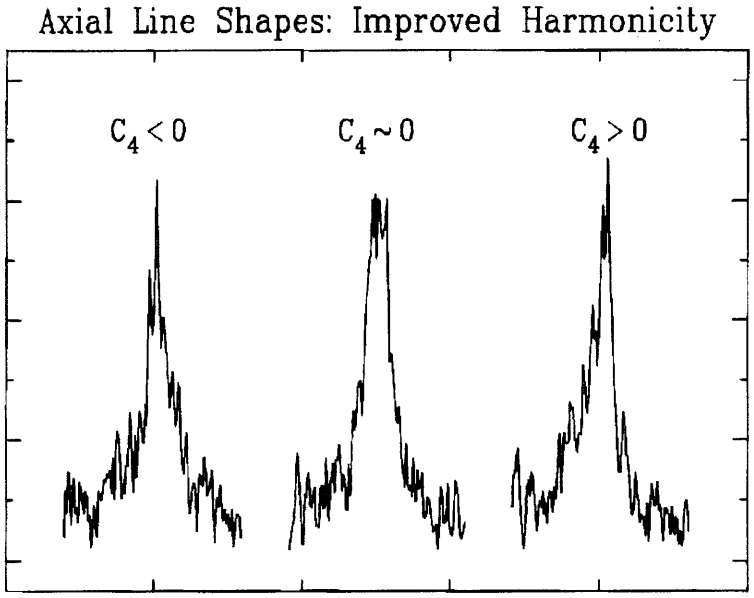

Figure 23.14

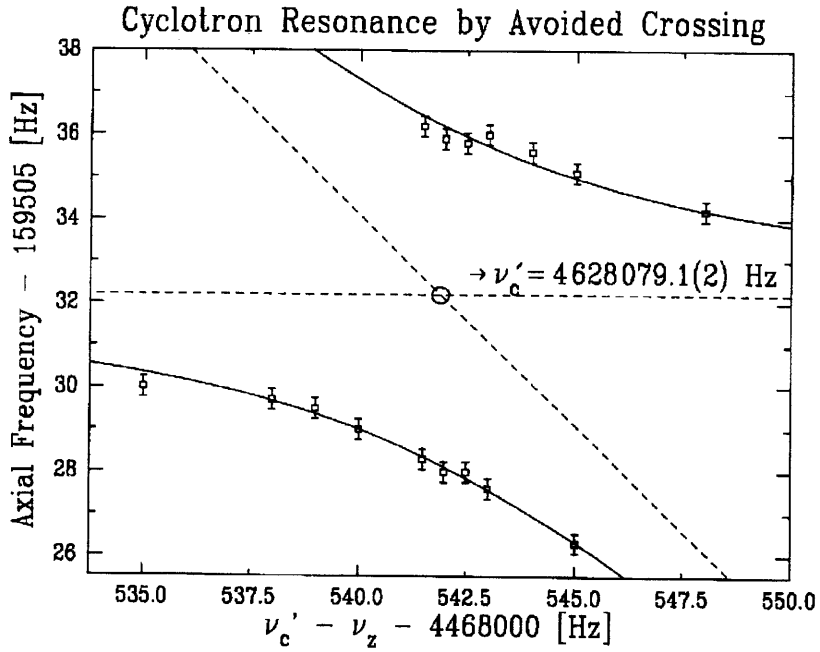

Figure 23.15

23.2.4 Experimental Study of Momentum Transfer to Atoms by Light

National Science Foundation (Grant PHY 86-05893)

David W. Keith, Bruce G. Oldaker, Andrew H. Miklich, David E. Pritchard

We are investigating the radiative forces experienced by a two-level atom interacting with light. These forces provide a new way to study the fundamental interaction between atoms and radiation, and also have important applications in the slowing, cooling, and trapping of neutral atoms using light. By deflecting a highly collimated (0.7 $\hbar$ FWHM resolution), state-selected, and velocity selected (11% FWHM) atomic sodium beam with a well-characterized light wave, we are able to make quantitative measurements of many aspects of momentum transfer to atoms by light. The transverse momentum resolution gives us the only apparatus in the world capable of single photon resolution.

Emphasis this year has been on momentum transfer by a standing wave. Here the momentum transfer can be viewed in terms of a classical force (the dipole force) which arises from the interaction of the induced electric dipole moment with the gradient of the standing-wave electric field. If the laser is detuned far enough from resonance, spontaneous emission is negligible and the process can be described by a semi-classical Hamiltonian. The momentum transfer can also be described as absorption/stimulated emission of photon pairs from the two counterpropagating traveling waves which make up the standing wave (see figure 23.16), a view which predicts momentum transfer in discrete units of 2 $\hbar$k as we observed. If the standing wave is considered as a grating, 2 $\hbar$k is the reciprocal lattice vector in which momentum is transferred if the grating is not excited.

The major breakthrough this year has been the observation of Bragg scattering of atomic waves off a standing wave light "crystal." If the atomic beam is viewed as a plane wave and the antinodes of the standing wave define crystal planes, then large resonances for momentum transfer occur for incident angles, θ , satisfying the Bragg law,

$$2d \sin\theta = n\lambda_{D.B.}, \text{ where } d = \frac{\lambda_{light}}{2}, \lambda_{D.B.} = \frac{h}{mv}$$

is the DeBroglie wavelength of the atomic wave, and n is an integer (see figures 23.17 and 23.18).[1]

Evidence of this new phenomenon opens up new possibilities for the construction of an "atomic interferometer;" basically, a device that interferes atomic waves.

Reference

[1] P.J. Martin, B.G. Oldaker, A.H. Miklich, and D.E. Pritchard, *Phys. Rev. Lett.* 60:515 (1988).

Publication

Pritchard, D.E., and P.L. Gould, *J. Opt. Soc. Am. B* 2:1799 (1985).

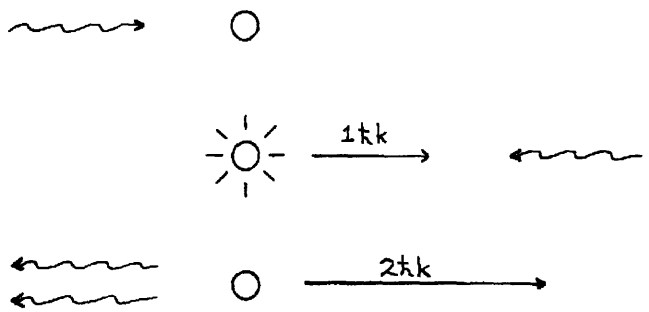

Figure 23.16 This shows schematically the absorption/stimulated emission process. a) Atom at rest absorbs a photon and 1 $\hbar$k of momentum. b) A photon from the counterpropagating traveling wave causes stimulated emission by the excited atom. c) Atom in ground state moves with 2 $\hbar$k of momentum and a photon has been traded from one traveling wave to the other.

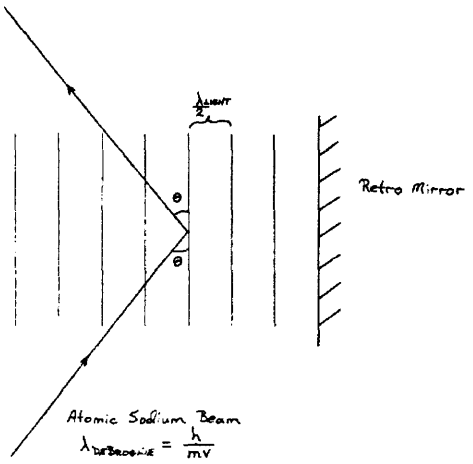

Figure 23.17 Schematic of Bragg scattering of an atomic sodium wave off a standing light wave.

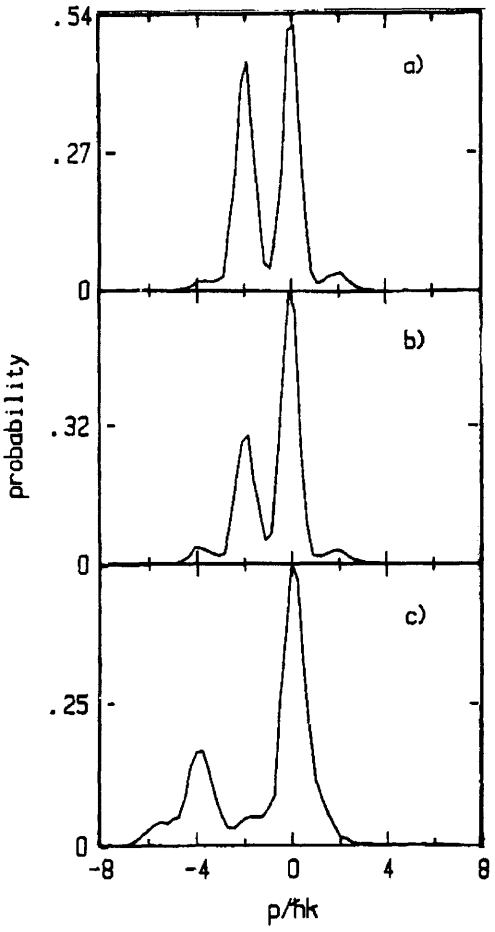

a) First order Bragg scattering: P = 6 mW; D = 800 MHz, t = 6.4 ms (DW = 3.2 mm).

b) First order Bragg scattering: P = 10mW; D = 800 MHz; t = 6.4 ms.

c) Second order Bragg scattering: P = 4mW; D = 500 MHz; t = 3.2 ms (DW = 1.6 mm). The angle of the standing light wave nodes with respect to the atomic beam was 30 mrad times the order, m.

Figure 23.18 Experimental data of Bragg scattering.